Conformational Self-Recognition as the Origin of Dewetting in Bistable Molecular Surfaces

Massimiliano Cavallini, Roberto Lazzaroni,† Roberto Zamboni, and Fabio Biscarini*

Consiglio Nazionale delle Ricerche - Istituto di Spettroscopia Molecolare, Via P. Gobetti 101, I-40129 Bologna, Italy

Dirk Timpel and Francesco Zerbetto*

Dipartimento di Chimica "G. Ciamician", Universitá degli Studi di Bologna, V. F. Selmi 2, I-40126 Bologna, Italy

Guy J. Clarkson and David A. Leigh*

Centre for Supramolecular and Macromolecular Chemistry, Department of Chemistry, University of Warwick, Coventry CV4 7AL, U.K.

Received: April 18, 2001; In Final Form: July 16, 2001

A thin film formed by an amphiphilic catenane is shown to exhibit bistable behavior. The film is grown by self-assembly from two different solutions onto a mica surface. Self-recognition of the solute molecules by the first monolayer of the adsorbed molecules drives the switch between two co-conformations, characterized by different polar character, which are nearly degenerate once deposited on the surface. The phenomenon takes the form of a wetting/dewetting transition and propagates the intramolecular change to the mesoscopic scale.

I. Introduction

Surface functionalization is an essential aspect in the development of materials interacting with their environment, which has direct relevance in areas such as sensing technologies. It is highly desirable that functional surfaces have a broad range of responses, while maintaining high sensitivity and selectivity. Materials which possess intrinsic multistability are ideally suited for fulfilling such requirements. In fact, reversible changes between different stable configurations can be triggered by external stimuli (chemical, mechanical, electrical, radiative). This opens a further potential, which is addressability of the functional surface.

The demonstration of the existence of thin films with an adaptive response to the environment is crucial to the development of functional surfaces and coatings. A functional surface requires systems capable of multistability with relatively low interconversion barriers between the different forms. A unimolecular example of this behavior in fluid media is the amphiphilic catenane, **1**,[1] which displays a novel form of environment-sensitive structural isomerism in which its polar groups are either exposed outside or buried inside the molecular core as a response to the nature of the solvent. The phenomenon is called "co-conformational" [2] switching (Figure 1), where the term "co-conformation" refers to the relative positions and orientations of mechanically interlocked components with respect to each other. Here we show that when this catenane is adsorbed on mica it provides the first example of bistable behavior on a surface, which manifests itself in a wetting/dewetting morphological transition. The mica surface nearly equalizes the energies of two co-conformations of the catenane so that the molecules adsorbed on the surface can switch through the interaction with other adsorbing molecules from the solution. The resulting loss of anchoring causes dewetting. Our system is a striking example of conformational recognition at a surface.

Binding interactions control the ordered arrangement of molecules on a surface, such as in self-assembly monolayers[3] and in epitaxial growth.[4−6] Conversely, the competition between attractive and repulsive interactions, such as in the case of phase segregation[7] and dewetting,[8,9]can be used to generate motifs and patterns with a characteristic length scale.[10] The combination of both features into a thin film is an attractive proposition for functional surfaces. The film could be switched at different length scales via an external stimulus and information stored through local changes of either order parameters or morphology.

In this context, benzylic amide catenanes[1,11−14] made of interlocking macrocycles are appealing since:

(i) they can be synthesized with a variety of functional groups;[11]

(ii) they form stacks ordered by intermolecular hydrogen bonds;[12]

(iii) their mechanical—not chemical—bond between the two macrocycles acts as a hinge for large amplitude submolecular movements, i.e. the rotation of one macrocycle through the cavity of the other or circumrotation;[13]

(iv) circumrotation can expose different functional groups (Figure 1) and, hence, the shell of outer interactions can be changed by controlling the circumrotation;

(v) catenanes can exhibit quasi-degenerate co-conformational energy minima, which may prelude to a multistable response[14] with energy barriers $\ll$20 kcal mol^{-1}.

These properties, especially iv and v, could be exploited in order to modify the interaction with a surface and give rise to dramatic morphological changes with the creation of domains and patterns.[15]

* Corresponding authors. For experimental, F.B. (e-mail, F.Biscarini@ism.bo.cnr.it); simulations, F.Z. (e-mail, gatto@ciam.unibo.it); synthesis, D.A.L. (e-mail, david.leigh@warwick.ac.uk).

† Permanent address: Service de Chimie des Matériaux Nouveaux, Université de Mons-Hainaut, Mons, B-7000 Belgium.

10.1021/jp011455t CCC: $20.00
Published on Web 10/11/2001

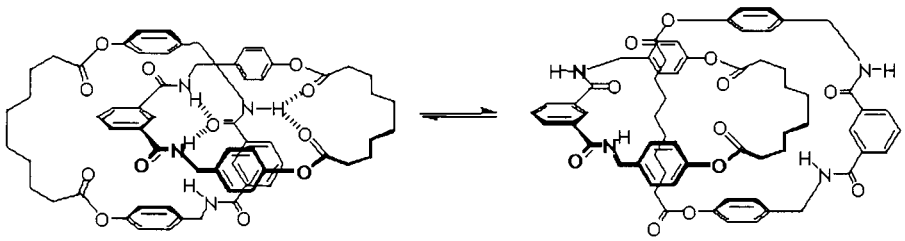

1a *1b*

Figure 1. Two principal co-conformations adopted by the amphiphilic catenane **1**: **1a**, alkyl chains exposed to the surface; **1b**, hydrogen bonding amide groups exposed to the surface. Co-conformation **1a** is dominant in the crystal and in non-hydrogen bonding solvents, **1b** in hydrogen-bond forming solvents.

Here we report a bistable behavior of catenane **1** which occurs during the self-assembly of the film on a polar surface. We explain the molecular origin of a wetting/dewetting transition in terms of the co-conformational changes of molecules in the adsorbed layer, which are controlled by the co-conformation of molecules in the solution.

II. Experimental Section

In chloroform, a non-hydrogen bonding solvent, the alkyl segments (eight methylene units) are exposed outside, and the rings are locked in position by bifurcated hydrogen bonds (see Figure 1a). A similar co-conformation is adopted in the crystal. In acetone, a hydrogen bond-forming solvent, the alkyl segments are buried inside the molecular core, and co-conformation **1b** with two polar amide groups protruding outward is dominant.

Films of **1** are grown by self-assembly, either from chloroform or acetone solutions (concentration range from 1 mM to 50 μM) onto freshly cleaved mica. The clean surface of mica consists of negatively charged O atom sheets, partially balanced by the potassium counterions. Mica is immersed in the catenane solution and kept in a closed ampule for increasing times ranging from minutes to a couple of days. After careful extraction and rinsing, the film is imaged by atomic force microscopy (AFM) in contact mode.

III. Results and Discussion

Figure 2a shows the formation of a monolayer from acetone solution. The height of the film with respect to the bottom of the voids (1 nm) and the sharp edges both suggest that the molecules are orderly arranged. AFM imaging at smaller scales (Figure 3a) reveals a rhombohedral mesh (2D Fast Fourier Transform, left inset), with 0.8 nm periodicity, and angles equal to 100° and 80°, respectively, distinct from the mica mesh (Figure 3b) (hexagonal, 0.5 nm periodicity, center inset). The periodicity observed is smaller than the intermolecular distance between nearest neighbors (1.2 nm) in the *ab* plane of the crystal[1], but the angles are within 10% of the crystal values (108° and 72°, respectively). The coating is smooth and featureless also when the deposition occurs from a chloroform solution, and the structure resolved by AFM (Figure 3c) reveals periodicity (0.85 nm) and angles (104° and 76°) comparable to those of the film from acetone. The similarities between the two films make us infer that the interaction with mica, rather than the solvent, controls the co-conformation of the molecules adsorbed in the first monolayer.

Above the monolayer, the evolution of the film morphology versus the amount of deposited material strongly differs in the two cases. Thin film growth from the acetone solution—where

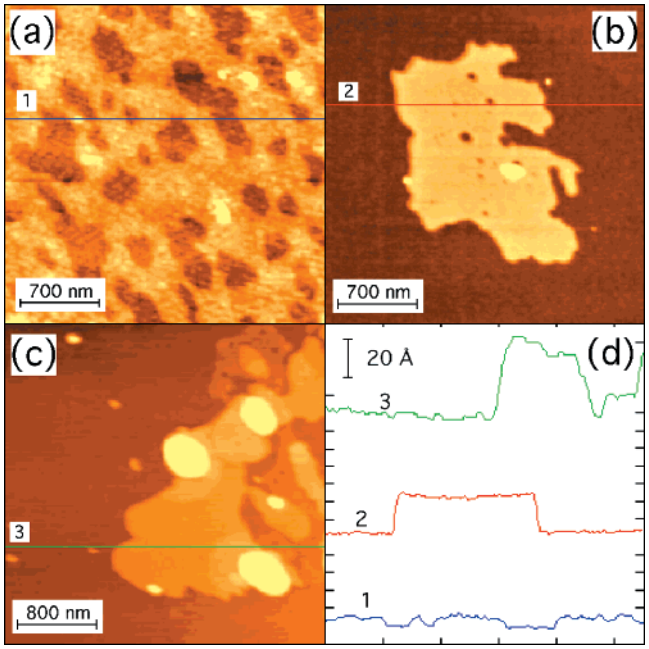

Figure 2. AFM topographical images of the morphology of **1** thin films deposited from an acetone solution (1 mM) for different times: (a) after 20′ min (b) after 2 h, (c) and 24 h. Terrace height is 1 nm, as from the profiles shown in panel d.

the catenane polar groups point outside, (**1b**)—proceeds with the stacking of monomolecular terraces (Figure 2b,c) whose steps are 1 nm high (Figure 2d). No reorganization of **1** is required at any stage of the growth process since both mica and acetone stabilize the same co-conformation (**1b**). We expect this layer to have a different structure compared to the reported crystal form,[1] where the polar groups are buried inside.

The morphology of the film grown from the chloroform solution changes dramatically as more material settles down from the solution. After the first monolayer is completed, the film starts rupturing and becomes "holey" as material recedes from the holes to the rims (Figure 4a). The rims exhibit the same height (approximately 2 nm) throughout the sample. A ballpark figure of the coverage at which the film rupture sets in may be given by estimating the ratio between the volume of the rim V_{rim} and the area A_{rim} bound by the outer rim. This yields a coverage of about 1.5 monolayers. We therefore estimate that the rupture sets in when the amount of deposited material is between 1 and 1.5 monolayers. At a later time (Figure 4b), holes grow larger by coalescence, while smaller holes appear in the interstitial region where material is re-deposited. The iteration of such processes is clear from Figure 4c,d where stacks of ruptured layers with different hole sizes are visible. After 48 h (Figure 4e), the film is completely ruptured into fragments of

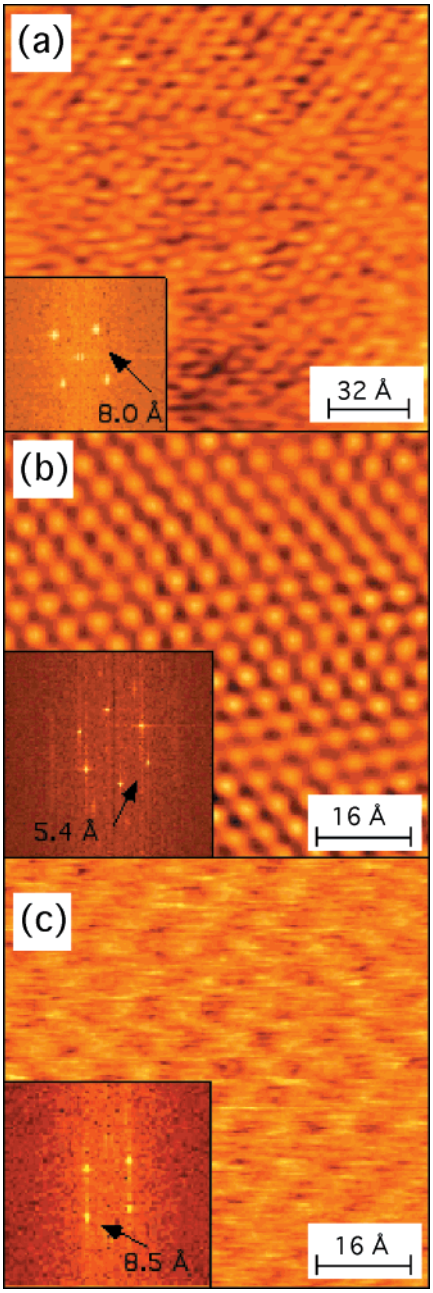

Figure 3. AFM error-signal images showing high-resolution details of (a) a **1** film deposited from acetone ($t = 20'$), (b) freshly cleaved mica prior deposition, and (c) a **1** film deposited from a chloroform solution ($t = 20'$). In the insets, the 2D fast Fourier transforms show bright spots corresponding to a wavelength of 0.8 nm for both **1** films and 0.5 nm for the mica mesh.

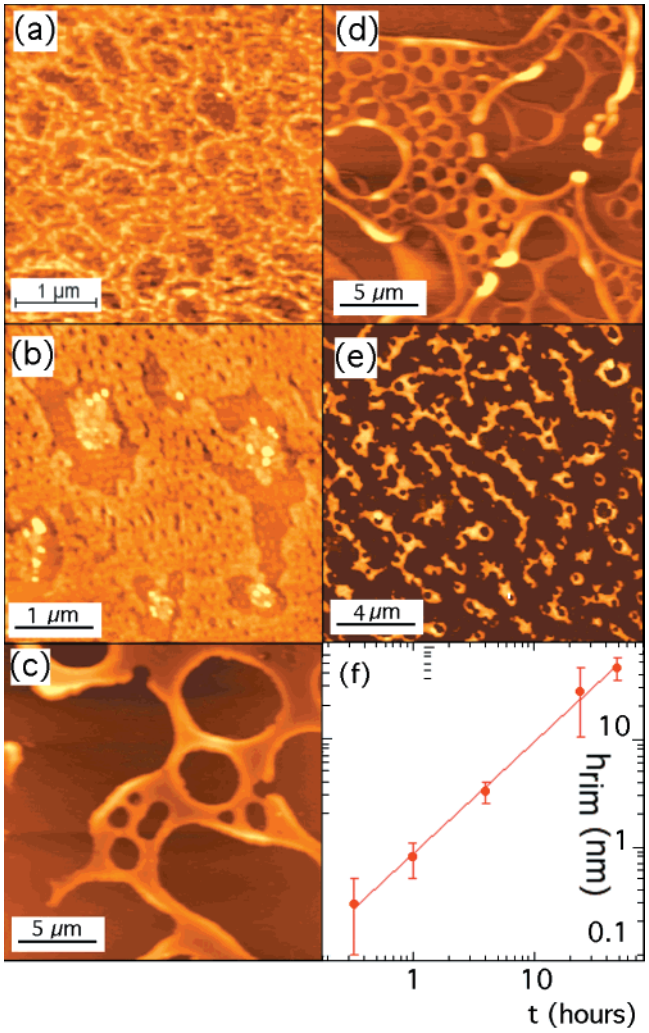

Figure 4. AFM images of the morphology of **1** film deposited from a chloroform solution (1 mM) after (a) 20′ min (height range $z = 0-2.2$ nm), (b) 1 h ($z = 0-8.0$ nm), (c) 4 h ($z = 0-100.0$ nm), (d) 24 h ($z = 0-100.0$ nm), and (e) 48 h ($z = 0-80.0$ nm); (f) plot of the height of the rims vs deposition time. Power-law fit (solid line) yields an exponent equal to 0.99 ± 0.03.

rims with uniform height. The height of the elevated rim, plotted in Figure 4f, with respect to the background grows linearly in time.

Rupture of a thin film by growing holes is one of the basic mechanisms of dewetting.[16] However, there are several interesting features in the case of **1** on mica:

(i) The spatial distribution of holes in Figure 4 and the fact that dewetting is only observed in the films deposited by chloroform suggest that the nucleation of holes is triggered by the material depositing from the solution, rather than by defects on the surface[17] or by the evaporating solvent.[18] This is somewhat reminiscent of the observation in ref 19, where dewetting in a polymer film is triggered by interactions with condensing water.

(ii) Molecules keep assembling from the solution onto the surface so that the mass of the system is not conserved. Holes are repeatedly filled with molecules until the monolayer ruptures. Iterated cycles of deposition−rupture−coalescence generate a hierarchy of holes.

(iii) The time scaling $h_{rim} \propto t$ is larger than the scaling $\propto t^{0.3-0.5}$ predicted in the case of dewetting of cast polymer films.[16,19,20]

An intuitive explanation of the larger exponent can be given in terms of the nonconservation of mass in this experiment, as opposed to the cast films, where mass is conserved. In the latter case, the relation between the height of the rim h_{rim} and hole radius R can be deduced by assuming that a toroid with a spherical cap section is formed as the material recedes from the monolayer to the rim. For a constant contact angle θ, the volume of the displaced monolayer equals the volume of the rim $V_{rim} = [\pi/(4 \sin \theta)]h_{rim}A_{rim}$ to yield $R^2/(b^2 + 2bR) = [\pi/(4 \sin \theta)](h_{rim}/h)$. Here h is the height of the monolayer, b is the base width of the toroid around the hole, and $A_{rim} = \pi[b^2 + 2Rb]$ is the area of the rim in contact with the surface. For $R/b \gg 1$, $R = [\pi/(2 \sin \theta)][bh_{rim}/h] = \pi\rho^2(1 - \cos \theta)/h$, with ρ as the radius of curvature of the toroid section. It turns out that for $R \propto t^{\beta}$, $h_{rim} \propto t^{\beta/2}$. If the mass is not conserved, a constant flux Φ makes the number N of molecules deposited over a circular patch of radius $R(t)$ to be $N =$

$\pi\Phi\kappa\int_0^t dt' R^2(t') \approx [\pi\Phi\kappa/(2\beta + 1)]t^{2\beta+1}$. Here κ is a constant, and the power-law evolution of R is a phenomenological approximation based on ref 20. Since $V_{rim} = NV_{mol}$, the constant being the volume of a molecule, it turns out that $V_{rim} \propto t^{2\beta+1}$; therefore, $h_{rim} \propto t^{\beta/2+0.25}$. In the case of viscous dissipation within the rim (no-slip conditions), $\beta = 1$, and $h_{rim} \propto t^{0.75}$, which confirms the trend observed in our case.

A similar phenomenology occurs for deposition onto the apolar freshly cleaved graphite surface, but for reverted solvent polarity. Moreover, we observe dewetting after deposition of a submonolayer from acetone onto mica (as in Figure 2a), followed by deposition from a chloroform solution. All these point to the fact that the transition from a wetting to a dewetting layer occurs when the co-conformation of molecules on the monolayer is mismatched with respect to the co-conformation in the solution. The evolution of the films deposited from chloroform solution (Figure 4) can be explained in terms of a first wetting monolayer which is stable on mica but becomes unstable as more molecules adsorb on top. The energy increase corresponding to the loss of interaction between the organic layer and the substrate should be compensated by the increased stability within the rim as strong packing interactions establish. This requires a co-conformational change of molecules in the first monolayer from **1b** to **1a**. Thus, dewetting is driven by the molecules in the **1a** form in the solution.

To understand the nature of the dewetting of **1** on mica, we set up model calculations on a simplified muscovite mica structure.[21−22] The mica model was implemented by substituting Mg atoms by Si/Al. Charge equilibrium was reached by choosing the adequate Si/Al ratio. An extended surface structure of $8 \times 8 \times 1$ unit cells was computer generated by extending the system in the *z*-direction. The oxygen-terminated surface was covered by half a layer of potassium atoms both on top and at the bottom. The atomic interactions within the structure were described by a simple Born−Mayer potential with dispersion term. The parameters for mica were taken from a data set which was fitted to ab initio calculations of silicas, aluminophosphates, and zeolites.[23] The Coulomb forces were treated with the Ewald summation technique. To increase the quality of the strong Coulombic catenane-mica interactions, the CO dipoles were substituted by partial charges on the two atoms. To speed up the calculations, an interaction list was used, and only the topmost Si/Al, O, and K layers were subjected to dynamics with the positions of all the other atoms frozen. The interaction between the substrate and the molecule was simulated by charge−charge and charge−dipole terms and a simple repulsive Born−Mayer term. The parameters were fitted according to the ionic radii of the different atom types. The simulations were performed with the MM3 model[24] implemented in the TINKER program [25] that has been successfully used to study catenanes and related systems.[12,13,25,26]

The two structural co-conformers **1a** and **1b** were investigated: in **1a**, the polar groups are buried inside, and the hydrogen bonds are formed between the two macrocycles; in **1b**, the polar groups are pointing outside and can form stabilizing interactions with the mica surface. To find the minimum energy configurations, molecular structural optimizations as well as "simulated annealing" procedures were carried out. In the case of the isolated molecule, the intramolecular hydrogen bonded network makes **1a** 13.8 kcal/mol more stable than **1b.** Figure 5a,b shows a view of the structures of **1a** and **1b** on mica, whose respective adsorption energies are ~58.1 and 82.3 kcal/mol. The adsorption on mica does not substantially change the intrinsic energies of the respective mica structures, which differ only by

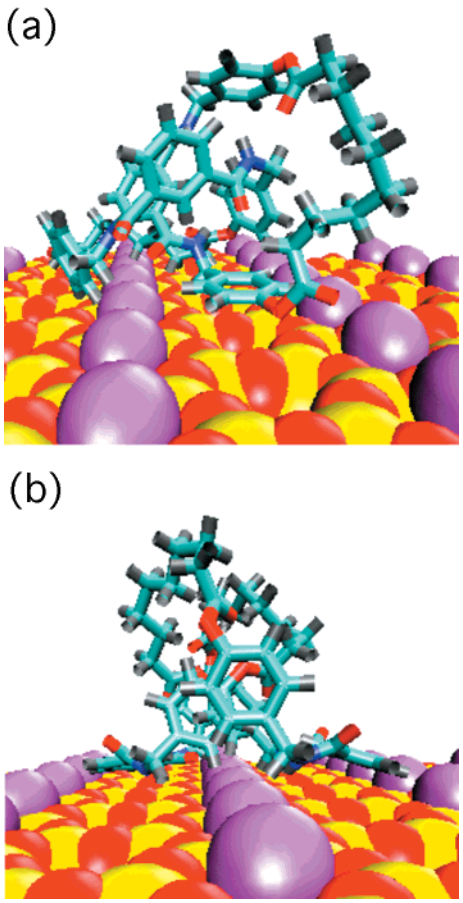

Figure 5. Optimized forms of catenane (a) **1a** and (b) **1b** on mica; O atoms are in red, N blue, C light-blue, H black, Si yellow, and K purple.

2.5 kcal/mol. The net result is that **1b** plus mica is 7.2 kcal/mol more stable than **1a** plus mica. Several points are worth emphasizing:

(i) On mica, the crystal-like structure **1a** is not the most stable.

(ii) The relatively small energy difference between **1a** and **1b** on the mica surface strongly hints to the possibility of creating a bistable system.

(iii) The creation of such a solid-state bistability could be reached once the system departs from the monolayer regime and approaches a multilayered crystal-like organization.

(iv) The work required to convert **1b** into **1a** originates from the packing energy difference of the two forms.

(v) In agreement with the general expectations for hydrogen bonded systems, packing energies of benzylic amide derivatives have been found to range substantially between 52 and 93 kcal/mol.[27]

As a consequence, it can be confidently suggested that the reorganization of the adsorbed **1b** form to the **1a** driven by **1a** molecules adsorbing from the chloroform solution occurs at the expense of the interaction with the surface, which results in dewetting. While the energy variation from our calculations may not be entirely accurate and the presence of solvents may further modify it, the calculations can be taken as a strong indication that form **1b** must eventually evolve dynamically to **1a** on a time scale similar to that observed experimentally.

In Figure 6, we sketch the molecular scenario of the process. Two quasi-degenerate adsorption states of **1** are possible on mica (Figure 6a), with P and A representing polar and apolar regions within the macrocycle, respectively, in close proximity with the surface. The potential energy double-well represents the bistable regime achieved upon adsorption, with a slightly more stable

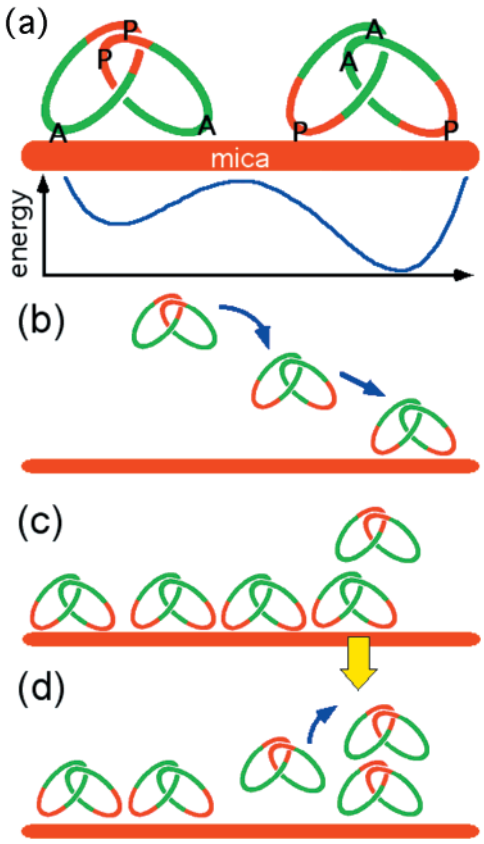

Figure 6. Proposed scenario for the molecularly controlled adsorption from **1a** chloroform solutions: (a) two quasi-degenerate adsorption states of **1** are possible on mica, with P and A representing polar and apolar regions within the macrocycle, respectively, in close proximity with the surface. The potential energy double-well represents the bistable regime achieved upon adsorption, with a slightly more stable situation when the polar regions are closer to the surface. (b) The adsorption of the molecules in the first monolayer from a chloroform solution. Molecules in co-conformation **1a** from the solution interconvert into **1b** upon adsorption. (c) **1a** molecules adsorbing at the second monolayer find a mismatched co-conformation **1b** in the first monolayer. (d) In order to minimize packing energy, incoming molecules **1a** induce the interconversion of **1b** molecules in the first monolayer into **1a**.

situation when the polar regions are closer to the surface. In Figure 6b, the adsorption of the molecules in the first monolayer from a chloroform solution is sketched. Molecules in co-conformation **1a** from the solution interconvert into **1b** upon adsorption. Then, **1a** molecules adsorbing at the second monolayer find a mismatched co-conformation **1b** in the first monolayer (Figure 6c). To minimize packing energy, incoming molecules **1a** induce the interconversion of **1b** molecules in the first monolayer into **1a** (Figure 6d). As a consequence, the bonding to the surface is weakened which, together with the presence of unsaturated dangling intermolecular H-bonds, generates dewetting.

It is clear that **1** has a dual behavior: it stabilizes the first adsorbed layer in the case of matching co-conformations of **1** in solution and on mica, while it promotes dewetting in the mismatched case. The same scenario, although with reverted solvent polarity—and possibly different co-conformers—occurs for self-assembly of **1** on the apolar graphite surface. The crucial finding conveyed here is that bistability of molecules can be created on a surface and can amplify its effects at length scales larger than that of the molecule itself through dramatic morphological changes. Importantly, the phenomenon described above could generate similar molecularly driven dewetting in a variety of complex molecular systems on surfaces when conjugated architectures, supramolecules, or biomolecules are incorporated in systems where two or more energy minima exist and the intramolecular interactions can compete with the surface interactions.

Acknowledgment. We thank J.-I. Pascual, G. Gadret, and G. Ruani for their help. We acknowledge partial support by EU-TMR Contracts ENBAC and DRUM (FMRX-CT96-0059 and FMRX-CT97-0097) and CNR-PFMSTA II-DEMO (post-doctoral fellowship for M.C.). D.A.L. is an EPSRC Advanced Research Fellow (AF/982324). R.L. is Maître de Recherches du Fonds National de la Recherche Scientifique (FNRS, Belgium).

References and Notes

(1) Leigh, D. A.; Moody, K.; Smart, J. P.; Watson, K. J.; Slawin, A. M. Z. *Angew. Chem., Int. Ed. Engl*. **1996**, *35*, 306.
(2) Fyfe, M. C. T.; Glink, P. T.; Menzer, S.; Stoddart, J. F.; White, A. J. P.; Williams, D. J. *Angew. Chem., Int. Ed. Engl.* **1997**, *36*, 2068.
(3) Ulman, A. *Chem. Rev*. **1996**, *96*, 1533 and refs therein.
(4) Forrest, S. R. *Chem. Rev*. **1997**, *97*, 1793.
(5) Umbach, E.; Sokolowski, M.; Fink, R. *Appl. Phys. A* **1996**, *63*, 565.
(6) Prato, S.; Floreano, L.; Cvetko, D.; De Renzi, V.; Morgante, A.; Modesti, S.; Biscarini, F.; Zamboni, R.; Taliani, C. *J. Phys. Chem. B* **1999**, *103*, 7788.
(7) Seul, M.; Andelman, D. *Science* **1995**, *267*, 476.
(8) Reiter, G. *Phys. Rev. Lett.* **1992**, *68*, 75.
(9) Brinkmann, M.; Biscarini, F.; Taliani, C.; Aiello, I.; Ghedini, M. *Phys. Rev. B Rapid Commun*. **2000**, *61*, R16339.
(10) Bowmann, C.; Newell, A. C. *Rev. Mod. Phys.* **1998**, *70*, 289.
(11) Johnston, A. G.; Leigh, D. A.; Nezhat, L.; Smart, J. P.; Deegan, M. D. *Angew. Chem., Int. Ed. Engl*. **1995**, *34*, 1212.
(12) Johnston, A. G.; Leigh, D. A.; Pritchard, R. J.; Deegan, M. D. *Angew. Chem., Int. Ed. Engl*. **1995**, *34*, 1209.
(13) Leigh, D. A.; Murphy, A.; Smart, J. P.; Deleuze, M. S.; Zerbetto, F. *J. Am. Chem. Soc.* **1998**, *120*, 6458.
(14) Caciuffo, R.; Degli Esposti, A.; Deleuze, M. S.; Leigh, D. A.; Murphy, A.; Paci, B.; Parker, S.; Zerbetto, F. *J. Chem. Phys.* **1998**, *109*, 11094.
(15) Reiter, G. *Langmuir* **1992**, *9*, 1344.
(16) Brochard-Wyart, F.; de Gennes, P.-G.; Hervert, H.; Redon, C. *Langmuir* **1994**, *10*, 1566.
(17) Jacob, K.; Herminghaus, S.; Mecke, K. R. *Langmuir* **1998**, *14*, 965.
(18) Hofkens, J.; Latterini, L.; Vanoppen, P.; Faes, H.; Jeuris, K.; De Feyter, S.; Kerimo, J.; Barbara, P.; De Schryver, F. C.; Rowan, A. E.; Nolte, R. J. M. *J. Phys. Chem. B* **1997**, *101*, 10588.
(19) Thiele, U.; Mertig, M.; Pompe, W. *Phys. Rev. Lett*. **1998**, *80*, 2869.
(20) Jacobs, K.; Seeman, R.; Schatz, G.; Herminghaus, S. *Langmuir* **1998**, *14*, 4961.
(21) Yerushalmi-Rozen, R.; Kerle, T.; Klein, J. *Science* **1999**, *285*, 1254.
(22) Pavese, A.; Ferraris, G.; Prencipe, M.; Ibberson, R. *Eur. J. Mineral.* **1997**, *9*, 1183.
(23) Kramer, G. J.; Farragher, N. P.; van Beest, B. W. H.; van Santen, R. A. *Phys. Rev. B* **1991**, *43*, 5068.
(24) Allinger, N. L.; Yuh, Y. H.; Lii, J.-H. *J. Am. Chem. Soc*. **1989**, *111*, 8551.
(25) Ponder, J. W.; Richards, F. M. *J. Comput. Chem.* **1987**, *8*, 1016.
(26) Deleuze, M. S.; Leigh, D. A.; Zerbetto, F. *J. Am. Chem. Soc*. **1999**, *121*, 1, 2364.
(27) Bermudez, V.; Capron, N.; Torsten, G.; Gatti, F. G.; Kajzar, F.; Leigh, D. A.; Zerbetto, F.; Zhang, S. *Nature* **2000**, *406*, 608.
(28) Leigh, D. A.; Leon, S.; Zerbetto, F. Manuscript in preparation. The smallest packing energy difference between two structures (21 kcal/mol) was determined for a fumaric acid derivative which differed only in the solvent included in the structure.